Canadian Science Publishing | Canadian Geotechnical Journal

Modelling Bio-geochemical Clogging affecting Piezometers in Acid Sulfate Soil Terrain

Journal:	*Canadian Geotechnical Journal*
Manuscript ID	cgj-2023-0004.R1
Manuscript Type:	Article
Date Submitted by the Author:	10-Apr-2023
Complete List of Authors:	Athuraliya, Senura; University of Technology Sydney Indraratna, Buddhima; University of Technology Sydney Medawela, Subhani; University of Technology Sydney Rowe, R. Kerry; Queen's University Thamwattana, Natalie; The University of Newcastle
Is the invited manuscript for consideration in a Special Issue? :	Not applicable (regular submission)
Keyword:	Piezometers, Acid sulfate soils, Bio-geochemical clogging, Excess pore water pressure

Modelling Bio-geochemical Clogging affecting Piezometers in Acid Sulfate Soil Terrain

Senura Athuraliya
PhD Candidate
Transport Research Centre,
School of Civil and Environmental Engineering,
Faculty of Engineering and Information Technology,
University of Technology Sydney, NSW 2007, Australia
Email: senura.h.athuraliya@student.uts.edu.au

Buddhima Indraratna*
Ph.D., FTSE, FIEAust., F.ASCE, FGS, CEng., CPEng.,
Distinguished Professor of Civil Engineering and Director,
Transport Research Centre,
Faculty of Engineering and Information Technology
University of Technology Sydney, NSW 2007, Australia
*Corresponding Author: Email: buddhima.indraratna@uts.edu.au

Subhani Medawela, Ph.D.,
Research Fellow
Transport Research Centre,
School of Civil and Environmental Engineering,
Faculty of Engineering and Information Technology
University of Technology Sydney, NSW 2007, Australia
Email: subhani.medawela@uts.edu.au

R. Kerry Rowe
OC, Ph.D., NAE, FRS, Dist.M.ASCE, P.Eng., CPEng.,
Barrington Batchelor Distinguished University Professor and Canada Research Chair in Geotechnical and Geoenvironmental Engineering,
Dept. of Civil Engineering, GeoEngineering Centre,
Queen's-RMC, Queen's Univ., Kingston, ON, Canada K7L 3N6
Email: kerry@civil.queensu.ca

Natalie Thamwattana, Ph.D.,
Professor of Applied Mathematics,
College of Engineering, Science and Environment,
School of Information and Physical Sciences
University of Newcastle, University Drive, Callaghan, NSW 2308, Australia.
Email: natalie.thamwattana@newcastle.edu.au

Total word count: 10,426

Abstract

This study offers an analytical solution for radial consolidation that captures the bio-geochemical clogging effect in acid sulfate soils. Field sites and personal communication with industry practitioners have provided evidence of piezometers exhibiting retarded pore pressure readings that do not follow conventional soil consolidation and seepage principles when installed in coastal acidic floodplains. This retarded response together with a variation in pH, ion concentrations, and piezometric heads provided evidence of clogging at and around the piezometers. This paper uses the proposed bio-geochemical clogging model, which is an analytically derived system of equations to estimate the excess pore water pressure (EPWP) dissipation of piezometers installed in clogging-prone acid sulfate soils. The inclusion of the total porosity reduction attributed to biological and geochemical clogging improves the predictions of the retarded dissipation of excess pore pressure, especially after about 1 year. This method is validated for two previously identified acidic field sites in coastal Australia, where piezometers measured a very slow rate of dissipation. It is concluded that this model has potential to accurately monitor the performance of critical infrastructure such as dams and embankment foundations built on acidic terrain.

Keywords

Piezometers, Acid sulfate soils, Bio-geochemical clogging, Excess pore water pressure

1 Introduction

Field instruments are essential tools used to take readings and measurements that assist during design, construction, investigations, monitoring and operation in geotechnical engineering. Measuring accurate and reliable pore water pressure measurements using piezometers has been a crucial part of this process and has been fundamental in performance monitoring of numerous geotechnical infrastructures (Arulrajah et al. 2004; Baral et al. 2021; Indraratna et al. 1992; Liu et al. 2005; Liu et al. 2007) and in geoenvironmental applications (Beaven et al. 2007; Gibert et al. 2019; Medawela et al. 2022).

Acid sulfate soils are considered problematic, as it contains environmentally hazardous sulfidic material (known as pyrite – FeS_2) that can partially oxidise and generate sulfuric acid. These low-lying sediments are commonly located in saturated ground environments comprised of a shallow groundwater table. These pyritic soils can often generate highly acidic conditions (pH ≈ 3-4), which may then lead to the mobilisation of metals such as Fe and Al into the groundwater at concentrations exceeding the permissible limits (e.g., Australian and New Zealand Guidelines for Fresh and Marine Water Quality, (ANZECC 2000)). These high metal concentrations are toxic to flora and fauna (Bigham and Nordstrom 2000; Dent and Pons 1995). The soluble Fe and Al can precipitate in nearby pore spaces reducing the porosity with time. Permeable reactive barriers (PRBs), a subsurface, porous treatment zone filled with reactive granular media, have been used for remediating contaminated acidic groundwater in acidic floodplains. Careful monitoring of the performance of these PRBs, using a comprehensive instrumentation framework (Medawela et al. 2022; Puls et al. 1999; Regmi et al. 2009) is important to ensure effective treatment. Piezometers play a vital role in a PRB monitoring network as the information related to variations in pore water pressures, hydraulic gradients and seepage flows are measured. However, the chemical precipitants and bacterial cells carried

by the contaminated groundwater accumulate in nearby pore spaces, such as piezometer filter tips, leading to false piezometer readings.

Gas generation or cavitation, extreme smearing of soil adjoining the filter, chemical alteration or corrosion of filter, electro-osmotic effects, soils with high clayey fractions, and filter tip clogging are some of the main factors that can impact the longevity and reliability of piezometers (Dibiagio 1977; Dunnicliff 2008; Hvorslev 1951; Ren et al. 2022; Ren et al. 2020). Of all these factors, filter tip clogging due to biological and geochemical interactions can affect piezometer readings significantly in low-lying acidic terrain. Hvorslev (1951) was one of the first to propose that clogging of filter tip pores can increase the time lag and affect the long-term reliability of piezometer readings. However, since then, even though researchers have looked at potential de-airing systems (Little and Vail 1960; Marsland 1973) to minimise the possibility of measuring pore air pressure, piezometer filter clogging has not been investigated. Clogging of piezometers should be addressed to minimise the piezometric error in readings to effectively meet the demands of the instrument.

While there have been extensive field, laboratory and theoretical studies of the biologically induced chemical precipitation of granular material in leachate collection systems for landfills (Cooke and Rowe 2008; Fleming et al. 1999; Rowe et al. 2000; Vangulck and Rowe 2008; Yu and Rowe 2012), no such extensive study has attempted to explain time-dependent clogging by biological and geochemical mechanisms that hinder the functionality of a piezometer which produce erroneous readings. This paper provides a novel mathematical framework to model the time-dependent biological and geochemical clogging phenomenon of a piezometer filter tip using radial consolidation theory. The coupled clogging was evident from a PRB monitoring framework, inclusive of piezometers, which was located in a low-lying acidic floodplain in the Shoalhaven region, Australia.

2 Field Evidence for Clogging affecting Piezometers

A variety of types and designs of piezometers are used and referred to in geotechnical engineering (Dunnicliff 1993; Hanna 1985). The most commonly used piezometers are Vibrating Wire Piezometers (VWPs), given their rapid response time and ease of use in fully grouted installations. However, it has been reported that some of the vibrating wire piezometers (VWPs) have shown retarded excess pore water pressure readings, when installed within the pyrite oxidation zone in low-lying acid sulfate soils (Athuraliya 2017; Indraratna et al. 2017). Even with and without the presence of prefabricated vertical drains (PVD), excess pore water pressure (EPWP) had not dissipated as expected after a certain period of time, typically close to a year (Indraratna et al. 2018a). Apart from having the appropriate Apparent Opening Size (AOS) of the drain filter jacket to prevent clogging of the outer PVD core (Bergado et al. 1996; Bo and Choa 2004), the discharge capacities of geosynthetic PVDs are generally 10-20 times greater than what would normally be associated with partial clogging to adversely influence the rate of excess pore pressure dissipation (Baral et al. 2021; Bergado et al. 1996; Chu et al. 2004). Based on previous observations (Baral et al. 2019; Indraratna et al. 2018b), the response of piezometers in terms of EPWP dissipation trends has shown a distinct trilinear trend, as presented in Fig 1. The response of piezometers in the initial stage (up to 1 years) is reliable. However, in the second stage, a gradual retardation of the EPWP dissipation trends is observed due to the partial clogging of the piezometer filter tip. As a result, a large time lag may be required to establish equilibrium at the soil-filter interface. In the third and final stage (after approximately 2 years), the filter tip clogs excessively and as a result, EPWP readings can be near constant without any dissipation.

There has been some previous research that provides evidence of geochemical and biological material in acid sulfate soils in water wells (Deed and Preene 2015; Houben 2003; Mclaughlan et al. 1993), drainage systems (Fleming and Rowe 2004; Smith and Melville 2004;

Sterpejkowicz-Wersocki 2014) and reactive barriers (Indraratna et al. 2020), but detailed clogging of piezometers has not been investigated. However, there have been potential cases in recent literature where researchers and practising engineers have acknowledged the potential for piezometers to clog and produce erroneous readings when installed in certain problematic soils (Baral et al. 2021; Mehdizadeh and Fakharian 2015; Yangiev et al. 2021). According to Hvorslev (1951), clogging in piezometers can be mainly divided into three: physical clogging, chemical clogging and biological clogging. Physical clogging (i.e., sediments) takes place when fine sediment particles accumulate in the pore space surrounding the piezometer filter tip (Reddi et al. 2000). However, use of a sand filter annulus or the recent use of geo-fabric wrapping in standpipes, as well as VWPs can prevent physical clogging (Arulrajah et al. 2013), even though clogging by geochemical and biological mechanisms will continue to have an adverse impact on piezometers when installed in clogging-prone floodplains.

Several instruments that had malfunctioned when they were installed in acid sulfate soils include; multiparameter sensors used to monitor the groundwater quality (Fig. 2a), partially clogged 'Casagrande' type standpipe filter tips (Fig. 2b) extracted from the Shoalhaven acidic floodplain. Some of the vibrating wire piezometers (VWP) were exhumed after 1 year at different depths, from a trial embankment project in Ballina (Fig. 2c-2e), which was also located in a low-lying pyritic floodplain (pH of groundwater < 4 and high organic content in the clay up to 6%). For instance, VWPs extracted 1.5 years after installation within the pyrite zone was found to be totally clogged (Indraratna et al. 2017). This certainly explains why EPWP dissipation was not recorded at all in that location after about 1 year, even though significant settlements (consolidation) were still occurring in the clay foundation. The clogging of piezometers can produce erroneous readings, particularly VWPs, which cannot be backwashed compared to conventional standpipe piezometers. To further confirm the clogging material, the filter tips were analysed using scanning electron microscopy (SEM) coupled with

energy-dispersive X-ray spectroscopy (EDS) and Fe and Al bearing mineral precipitates prevalent in acidic floodplains were detected (Indraratna et al. 2018a). Iron oxy/hydroxides are one of the most commonly found mineral precipitates formed and block pore spaces in filter gravel and/or screen slots (Bustos Medina et al. 2013; Houben 2003). However, in Australia, it has been identified that Al hydroxides are also amongst the most abundant incrustations (Mclaughlan et al. 1993). These Al and Fe precipitates generally take a 'milky-white' and 'orange-brown' colour, respectively, as observed in laboratory column experiments using synthetic acidic groundwater by (Indraratna et al. 2020). Such encrustations and stains have appeared frequently in instrumentation installed in field sites that compose acid sulfate soils, as presented in Fig 2.

When installed in coastal acidic floodplains, numerous cases in which piezometers have produced retarded excess pore pressure readings that do not follow conventional soil consolidation and seepage principles have been reported (Baral et al. 2021; Indraratna et al. 2018a; Kelly et al. 2018; Nguyen et al. 2022). Even though piezometer malfunctioning has been detected in low-lying sites in the Shoalhaven and Ballina floodplains of Australia, research efforts to solve the problem have been minimal. This is the first time a mathematical framework has been used to capture the response of a piezometer that undergoes time-dependent biological and geochemical clogging. The following section elaborates on a particular study site where clogging in pyritic terrain was observed over the years.

3 Study Site

The main study site is located in the low-lying Shoalhaven floodplain, Bolong, New South Wales, Australia. A flood mitigation drain flows adjacent to the site and flows into Broughton Creek, a tributary of the Shoalhaven River. The site is located in a low-lying pyritic terrain with saturated clayey soil where the average depth of water table from the ground surface is

0.50-0.75 m. The groundwater is acidic, reaching average pH values of 3.7 and contains high concentrations of Al and Fe (Table 1). A pilot-scale permeable reactive barrier (PRB was installed at the site in 2006 to remediate the contaminated acidic groundwater from the site (Fig. 3). A geotechnical instrumentation framework (Fig. 4) was also installed at the site to monitor the performance of the PRB, which is used to treat acidic groundwater. Detailed construction procedures of the site instrumentation and monitoring framework, which includes several observation wells, standpipe piezometers, vibrating wire piezometers (VWPs) and multi-parameter sensors with data loggers, are presented in Medawela et al. (2022). In order to ensure the accurate measurement of pore pressure, the piezometer filter tips were properly saturated with deaired water prior to installation as suggested in ASTM (2020) and elaborated earlier by Take and Bolton (2003). This study mainly focuses on the impact of clogging on instrumentation, especially piezometers. Due to the variations in pH levels of the acidic groundwater, toxic metals such as Fe and Al can precipitate on nearby instrument surfaces. The observation wells and standpipe piezometers were installed adjacent to each other along the centreline of the PRB in order to investigate the impact of clogging surrounding the piezometer filter tips. Groundwater samples were collected monthly from these observation wells, and the water chemistry was measured, especially the dissolved concentrations of Al and Fe, to present the impact of clogging on piezometers in subsurface conditions, which is discussed in detail in section 3.2.

Recent variation in site pH levels can readily be observed by multi-parameter sensors and data loggers connected to the nearby creek (Fig. 5). The site consists of a cyclic variation of groundwater pH dependent on seasonal rainfall where a higher pH (average pH of 6.4) is typically observed soon after a major rainfall event, whilst acidic conditions prevail (average pH of 3.8) during dry periods. The study site is also located in a region prone to extreme variations in seasonal rainfall (e.g. > 200 mm/24 hour 10/02/2020 and 08/08/2020) and, as a

result, experiences accumulation of Fe and Al bearing minerals in sediments due to periodic oscillations in groundwater levels. The low-lying floodplain soil has remained below the water table for thousands of years since its deposition under water. It would have had larger water filled pores initially, but since that time it has undergone consolidation over many years and a reduction in voids ratio with no opportunity for air to enter the pores with further deposition, thus remaining saturated as also confirmed by microscopic examination (SEM) of undisturbed sampling of the deposits (Karimian et al. 2018; Medawela et al. 2022).

3.1 Bacterial Interaction in Clogging

The acidophilic microbial strain, *Acidithiobacillus ferrooxidans*, was identified to be the most common iron oxidising bacteria strain (IOB) in soil samples extracted from the study site through bacterial diversity profile analysis using nucleic acid extraction performed by the Australian Genomic Research Facility (AGRF, Australia). Detailed microbial analysis of the soil conducted at the site is presented in Indraratna et al. (2020). *A.Ferrooxidans* mainly contributes towards the formation of mineral precipitates in pyritic soils as well as acid mine drainage (Baker and Banfield 2003; Wang and Zhou 2012). In low pH environments (pH < 3.5), these iron oxidising bacteria can catalyse the oxidisation of Fe^{2+} to form ferric ions (Fe^{3+}) by more than 6 orders of magnitude, further enhancing the clogging of surrounding porous media (Singer and Stumm 1970). After the pyrite oxidation has commenced, Fe^{3+} can further oxidise, exacerbating the generation of acidity in soils (Eqs. 1-2). The bacteria can migrate through groundwater and come into contact with geotechnical instrumentation, such as vibrating wire piezometers installed in pyritic terrain. The biotic role in piezometer clogging is imperative as it can influence the clogging mechanism in two ways. Firstly, the iron oxidising bacteria can behave as a catalyst in the pyrite oxidation process (Eqn. 1), impacting the rate of mineral precipitation (Nordstrom 1982). Secondly, the growth of bacteria or biomass (bacterial

cells and Extra-cellular Polymeric Substances (EPS)) can fill the void spaces and clog the piezometer filter tip (Indraratna et al. 2018a).

$$Fe^{2+} + \frac{1}{4}\,O_{2(aq)} + H^{+} \xrightarrow{Bacteria} Fe^{3+} + \frac{1}{2}\,H_2O \quad (1)$$

$$FeS_{2(s)} + 14\,Fe^{3+} + 8H_2O \xrightarrow{Bacteria} 15\,Fe^{2+}_{(aq)} + 2\,SO_4^{2-} + 16\,H^{+} \quad (2)$$

3.2 Clogging effects on Piezometers at the Study Site

The impact of clogging on piezometers at the study site can be illustrated using the average measured variations in pH and concentrations of Fe and Al (Figs. 6-7). The pH and dissolved concentrations of Fe and Al of groundwater specimens were taken from different sections of the PRB, namely, inlet (0 – 0.4 m), central (0.4 – 0.8 m) and outlet (0.8 – 1.2 m) sections. Samples were collected using a bailer from observations wells (OWs) located in respective zones (inlet – OW18, OW21, OW25; central – OW20, OW22, OW24; outlet – OW17, OW19 and OW23). Each section of the PRB indicated an increased pH towards the outlet due to the neutralisation of the acidic groundwater by the barrier (Fig 6). The acidic groundwater front from the upgradient (pH ≈ 3.7) reacted with the inlet face of the barrier to produce bicarbonate (HCO_3^-) alkalinity (Eqs. 3-4). As a result, an initial pH of 6.4 was measured at the inlet. Considering the overall trend of pH variation (Day 0-740), the central and outlet sections mostly recorded a greater pH than the inlet since these adjacent sections were exposed to less acidic water.

$$CaCO_3 + 2H^{+} \longleftrightarrow Ca^{2+} + 3H_2CO_3 \quad (3)$$

$$CaCO_3 + H_2CO_3 \longleftrightarrow Ca^{2+} + 2\,HCO_3^{-} \quad (4)$$

Soon after the construction of the PRB, it acted as a sink, and the acidic groundwater flowed into the granular construction and exhibited a fluctuation in the pH. An initial peak in pH was observed due to the first flush of alkalinity produced by the dissolution of the

cementitious minerals in the recycled concrete aggregate (RCA). By day 220, the pH of all the sections had plateaued and stabilised, maintaining the general trend of producing the lowest pH at the inlet and the highest at the outlet section. The neutral pH (7.6<pH<7.8) observed from the outlet since day 240 can be attributed to the bicarbonate buffering where HCO_3^- ions are released (Eqs. 3-4). Similarly, (Indraratna et al. 2020) observed the bicarbonate alkalinity produced within 70 days in laboratory column tests, which were conducted in controlled and accelerated conditions.

The concentrations of Al and Fe were much lower for the PRB outlet section compared to the inlet, and the average concentration for both was below 0.4 mg/L (Fig. 7). The rate of change of concentration was much lower than the inlet and central sections. The significant reduction in dissolved Al and Fe concentrations within the outlet section infers that a large proportion has precipitated out of solution within the previous sections of the PRB in forms of oxides and hydroxides (Eqs. 5-8). Given that the descending order of Al and Fe concentrations observed was from inlet, central and outlet sections, respectively, the greatest proportion of precipitation is expected at the inlet section, similar to laboratory column test observations (Indraratna et al. 2020). However, seasonal changes in rainfall can have a significant impact on pH due to fluctuations in groundwater levels and the saturation of the PRB. This can further exacerbate the accumulation of various species of Fe and Al bearing minerals in surrounding sediments and instrumentation such as piezometers.

$$Fe^{3+} + 3\,H_2O \longrightarrow Fe(OH)_{3(s)} + 3\,H^+_{(aq)} \quad (5)$$

$$Fe^{3+} + 2\,H_2O \longrightarrow FeOOH + 3\,H^+_{(aq)} \quad (6)$$

$$2\,Fe^{3+} + 3\,H_2O \longrightarrow Fe_2O_3 + 6\,H^+_{(aq)} \quad (7)$$

$$Al^{3+} + 3\,H_2O \longrightarrow Al(OH)_{3(s)} + 3\,H^+_{(aq)} \quad (8)$$

The fluctuating pH within the acidic terrain controls the rate of Al and Fe precipitation, and given that piezometers are installed for prolonged periods, the filter tip and the immediate porous annulus would gradually build up with mineral precipitates. The average Al concentration for the duration of 750 days was 1.92 mg/L for the inlet section, 0.99 mg/L for the central section and 0.33 mg/L for the outlet section (Fig. 7b). The fluctuating variations of peaks and troughs in concentrations can be mainly attributed to the dynamic redox oscillations that are generally noticed in acid sulfate floodplains (Karimian et al. 2018). Similar to the pH variation of different sections within the PRB, clogging and armouring of mineral precipitates are non-uniform within the barrier and indicate that clogging capacity decreases towards the outlet (Medawela and Indraratna 2020).

As mineral precipitation and formation of biological material occur, the response of the piezometers is delayed due to a time lag (Indraratna et al. 2018a). The continuous reduction in pore space builds up the pressure head of the installed standpipe piezometers (P) of each section considered (inlet – P9 and P12; central – P7 and P10; outlet – P8 and P11) with respect to time (Fig. 8). The initial peak in piezometric head observed after 100 days appears to be due to the same first flush that produced alkalinity at the inlet where the pH level reached 9.4 (see Fig. 6). Furthermore, rapid rainfall events observed prior to day 100 would also contribute towards measuring a sudden peak in the piezometric head due to the infiltration that could have saturated the PRB. After 150 days, the average piezometric head of the inlet, central and outlet sections were 0.40 m, 0.39 m and 0.42 m, respectively. However, since then (day 150 – day 790), the piezometric head followed an increasing trend, where an average rise of 0.45 m, 0.38 m and 0.36 m were measured at the inlet, central and outlet sections, respectively. The greatest increase in head was observed at the inlet section, where clogging was most aggressive. The pore blockages and resulting obstruction of the flow paths of the piezometer filter tip were further evident when some of the piezometers were exhumed from the site, as presented in Fig.

(2). However, standpipe piezometers can be backwashed, which is desirable when they are installed in acid sulfate floodplains, to clear the blocked pores of the filter tip. This is not possible in the case of other piezometers, such as vibrating wire piezometers. Therefore, it is essential to simulate the performance of VW piezometers before installing them to ensure the safety of critical infrastructures such as dams and embankment foundations. For this purpose, a novel mathematical model is developed in the next section considering biological and geochemical clogging to interpret the dissipation of EPWP in acidic floodplains.

4 Mathematical Model Development

4.1 Modelling Biological Clogging in Porous Media

The growth of biomass/slime on geotechnical instruments has been reported, especially in organically rich soils (Easton and Springer 2016; Indraratna et al. 2018a), and these cells usually attach to the surfaces of filter tips and can multiply until the surface is completely smothered (Macdonald and Clark 1970; Ralph and Stevenson 1995). This study follows a macroscopic approach using properties such as porosity and hydraulic conductivity of the filter tips, where the pore morphology can be simulated without considering individual pores, but by considering the microbial activity in the entire porous section of influence (Chen-Charpentier 1999).

Using the macroscopic approach, the porosity reduction due to the acidophilic bacterial growth in the porous matrix surrounding the piezometer filter tip can be estimated by Eqs. (9-10) (Indraratna et al. 2020).

$$n_{t_b} = \frac{Xs}{\rho_c} \tag{9}$$

$$Xs = \frac{X_0 e^{k_c t}}{1 - \frac{X_0}{X_\infty}(1 - e^{k_c t})} \tag{10}$$

where n_{t_b} is the porosity reduction due to growth of biomass; Xs is the solid phase concentration of bacterial cells; ρ_c is the density of solid phase biomass; X_∞ is the maximum bacterial cell concentration; X_0 is the initial bacterial cell concentration k_c is the carrying capacity coefficient and t is time. Similar to Indraratna et al. (2020), the concentration of the bacterial cells were estimated using a logistic approach which assumes a sigmoidal-shaped growth curve to estimate the biological clogging that takes place within the reactive material of a PRB (Monod 1949; Shuler and Kargi 2002).

4.2 Modelling Chemical Clogging in Porous Media

The reduction in porosity due to secondary mineral precipitation can be given by Eqn. (11) (Steefel and Lasaga 1994).

$$\frac{\partial \emptyset_m}{\partial t} = \sum_{k=1}^{N_m} M_k R_k \tag{11}$$

where $\emptyset_m$ is the volume fraction of the mineral; M_k is the mineral molar volume ($m^3 mol$), R_k is the overall reaction rate of the mineral ($molm^3 s^{-1}$).

The change in temporal porosity due to chemical precipitates can then be obtained by Eqn. (12) (Indraratna et al. 2014).

$$n_{t_c} = \sum_{k=1}^{N_m} M_k R_k t \tag{12}$$

where n_{t_c} is the reduction in porosity due to secondary mineral precipitates; N_m is the number of minerals and $M_k R_k$ is the term that is continuous for a particular time step.

The biologically catalysed mineral precipitation and reactions that take place in acidic pyritic terrain can be presented using a coupled biological and geochemical algorithm. This algorithm consists of 6 reactions that consider the precipitation reactions (Table 2) that are assumed to be the dominant reactions that result in biological and geochemical clogging, as presented by Regmi et al. (2009). The primary contributors for the chemical precipitations have already been identified as Fe and Al bearing minerals with respect to the acidic floodplain (Indraratna et al. 2014; Regmi et al. 2009).

The precipitation of secondary mineral precipitates was assumed to follow transition state theory (TST) presented by Eqn. (13) and has been used successfully to determine the rate kinetics in granular assemblies (Indraratna et al. 2014; Li et al. 2006; Medawela and Indraratna 2020).

$$r_k = -k_r\left(1 - \frac{IAP}{K_{eq}}\right) \tag{13}$$

where r_k is the reaction rate of each component; k_r is the kinetic rate coefficient; IAP is the ion activity product, K_{eq} is the solubility constant for each reaction. The saturation indices (SIs) for precipitating minerals were calculated using PHREEQC software, which was based on the geochemistry of the groundwater (concentrations of Na^+, K^+, Ca^{2+}, Mg^{2+}, Al^{3+}, Fe^{3+}, Cl^- and SO_4^{2-}), pH and temperature (Regmi et al. 2011).

$$SI = \log(IAP) - \log(K_{eq}) \tag{14}$$

The biologically catalysed mineral precipitation (i.e., Eqn. 15), where the rate of microbial oxidation of Fe^{2+} into Fe^{3+} can be represented by the following equation:

$$\frac{d[Fe^{2+}]}{dt} = k_{bio}\left(\frac{[Fe^{2+}]}{k_{Fe^{2+}} + [Fe^{2+}]}\right)\left(\frac{[O_2]}{k_{O_2} + [O_2]}\right)\left(\frac{[H^+]}{k_{H^+} + [H^+]}\right) \tag{15}$$

where $[Fe^{2+}]$, $[O_2]$ and $[H^+]$ and $k_{Fe^{2+}}$, k_{O_2}, k_{H^+} are concentrations and half-saturation constants of ferrous ions, oxygen and hydrogen ions respectively, whilst k_{bio} is the kinetic rate coefficient of the biologically catalysed reaction. Further details of the bio-geochemical algorithm and the overall kinetics for each species are illustrated in Supplementary Material (Section A).

4.3 Modelling the Porosity Reduction

The reduction in hydraulic conductivity due to clogging was modelled using the Kozeny-Carman theory to predict the hydro-mechanical behaviour of the porous medium with porosity reduction due to clogging (Indraratna et al. 2020; Indraratna et al. 2014; Li et al. 2006; Rowe and Fleming 1998). The normalised Kozeny-Carman formulation is expressed by:

$$k = K_0 \left(\frac{n_0 - \Delta n_t}{n_0}\right)^3 \Big/ \left(\frac{1 - n_0 + \Delta n_t}{1 - n_0}\right)^2 \quad (16)$$

where K_0 is the initial hydraulic conductivity of the porous medium, n_0 is the initial porosity of a soil or granular medium.

The total porosity reduction (Δn_t) due to biomass accumulation (n_{t_b}) and chemical precipitation (n_{t_c}), can be given by:

$$\Delta n_t = n_{t_c} + n_{t_b} \quad (17)$$

Therefore, the resulting porosity at time t (n_t) can be expressed by:

$$n_t = n_0 - \left(n_{t_c} + n_{t_b}\right) \quad (18)$$

The reduction in total porosity (n_t) due to biologically catalysed chemical precipitation (n_{t_c}) and bacterial growth (n_{t_b}) within a porous matrix is presented by Eqn. 18. The variation of these factions with respect to time is presented in Fig. 9 for the inlet section of the PRB,

based on average field parameters of the study site (Table 1) and the overall kinetic rate coefficients (Table 2). Initially, the biological clogging (n_{t_b}) contributed towards 75% of the total porosity reduction, whilst the chemical precipitation (n_{t_c}) was limited to 25% within the first 100 days.

A rapid growth in bacterial cells can be predicted until approximately 250 days, after which the rate of porosity reduction due to biomass accumulation gradually slows down until it plateaus at approximately 65% of the total porosity reduction. The initial accelerated growth of bacterial cell mass at the inlet of the PRB can be attributed to the redundantly available substrate and ideal environmental conditions. Even though the conditions are favourable in acid sulfate terrain, according to the growth curves of biomass, a growth limit exists, as observed by Medawela et al. (2023) in laboratory column experiments. The decay in n_{t_b} was observed for the next 390 days and follows a typical sigmoidal shape of biomass growth (Shuler and Kargi 2002). The increase in mineral precipitation from day 250 may be due to the oxidation of Fe^{2+} to Fe^{3+} catalysed by bacterial species activated by field environment conditions. However, a continuous and gradual increase in n_{t_c} was observed for the entire 640 day period, by which 35% of the total porosity reduction was attributed to geochemical clogging. Therefore, this porosity reduction model implies that the accumulation of bacterial cell mass plays a significant role in reducing the pore space only at the initial stage, but later (after day 250), mineral precipitation takes over as the major clogging mechanism. The deposition of secondary mineral precipitates was further supported by a comprehensive mineralogical analysis (SEM-EDS) performed by Medawela et al. (2022), where the extracted aggregates displayed peaks in EDS diffractograms for respective Fe and Al-bearing minerals, when compared with fresh aggregate samples of the PRB. Similar observations were made in laboratory column experiments using granular media, where mineral precipitates had deposited within the column reducing the overall hydraulic conductivity and 68% reduction in porosity

of the column, when synthetic acidic groundwater was passed through which mimics the field groundwater chemistry at the inlet (Medawela et al. 2023).

The porosity change was calculated for the first 2 years, but for a longer time duration, mineral precipitation may have a greater impact on the total reduction in pore volume with the continuously fluctuating site conditions observed in the study site. For instance, Medawela et al. (2022) reported a continuous reduction in hydraulic conductivity caused by biologically catalysed mineral precipitation within the PRB over their monitoring period of 16 years. They also observed that the rate of reduction of hydraulic conductivity increased towards the end of the monitoring period, which they attributed to increased clogging and armouring. In essence, mineral precipitation is expected to continue over many years without attaining a perfectly stable state, due to the constantly fluctuating site conditions (pH, Fe and Al concentrations, rainfall, water table depth) and the corresponding intensity (density) of bacterial strains observed in the natural environment. In accelerated laboratory column tests, Medawela et al. (2023) observed a similar total porosity reduction, where geochemical clogging surpassed porosity reduction due to biological clogging after 190 days. After considering the porosity reduction model, the significance of including both chemical and biological interactions that take place during clogging is evident, in order to evaluate the overall porosity reduction of a porous medium.

5 Bio-geochemical Clogging Model considering Radial Consolidation

A novel mathematical framework was used in this study to capture the impact of biological and geochemical clogging on piezometer readings. The governing equation for excess pore water pressure (EPWP) dissipation in a saturated soil element of radial distance r and depth z considering both vertical and radial drainage can be expressed as (Barron 1948):

$$\frac{\partial u}{\partial t} = c_v\left(\frac{\partial^2 u}{\partial z^2}\right) + c_h\left(\frac{\partial^2 u}{\partial r^2} + \frac{1}{r}\frac{\partial u}{\partial r}\right) \quad (19)$$

where, u is the excess pore water pressure; t is time elapsed and c_v and c_h are the coefficients of consolidation in the vertical and radial directions, respectively. To further simplify, assuming radial flow only, the above equation can be denoted as:

$$\frac{\partial u}{\partial t} = c_h\left(\frac{\partial^2 u}{\partial r^2} + \frac{1}{r}\frac{\partial u}{\partial r}\right) \quad (20)$$

$$c_h = \frac{k}{m_v \gamma_w} \quad (21)$$

where k_h is hydraulic conductivity in the radial direction and m_v is the coefficient of volume compressibility.

Substituting Eqn. 21 in Eqn. 20, the governing relationship for consolidation theory for radial flow can be presented as:

$$\frac{\partial u}{\partial t} = \frac{k}{m_v \gamma_w}\left(\frac{\partial^2 u}{\partial r^2} + \frac{1}{r}\frac{\partial u}{\partial r}\right) \quad (22)$$

5.1 Analytical Solutions for Variations of Excess Pore Water Pressure over Time:

To develop the analytical solutions, it is assumed that the excess pore water pressure can be rewritten as a product of two independent functions (Eqn. 23), each of which depends on only radial distance r and time t, respectively. Therefore, the governing equations obtained can be solved by the variable separation method, where,

$$\overline{u}(r,t) = X(r).Y(t) \quad (23)$$

The governing equation can now be transformed into a Bessel Function in the form of

$$\overline{u} = [C_2 J_0(Ar) + C_3 Y_0(Ar)].e^{(F(t))} \quad (24)$$

where J_0 and Y_0 represent Bessel's functions of zero-order of the first and second kind, respectively.

The general analytical solution to Eqn. (19) for radial flow is given in the form of:

$$\overline{u}(r,t) = X(r).e^{F(t)} \tag{25}$$

where,

$$X(r) = \sum_{n=1}^{\infty} C_n J_0\left(\frac{\alpha_n r}{R_0}\right) \tag{26}$$

and

$$F(t) = \frac{-A^2}{B}\left(-\frac{\sum_{k=1}^{Nm} M_k R_k t^2}{2} + \frac{X_\infty}{\rho_c k_c} ln\left[1 - \frac{X_0}{X_\infty}(1 - e^{k_c t})\right] + (n_0 + 2)\, t - 3\, ln[f(t) - n_0 + 1] + 3\, ln\left[\frac{X_0}{\rho_c} - n_0 + 1\right] + \frac{1}{(f(t) - n_0 + 1)} - \frac{1}{\left(\frac{X_0}{\rho_c} - n_0 + 1\right)}\right) \tag{27}$$

where $C_n = \frac{2u_0}{\alpha_n J_1(\alpha_n)}$; $A = \frac{\alpha_n}{R_0}$; $B = \frac{m_v \gamma_w {n_0}^3}{K_0(1-n_0)^2}$ and

$$f(t) = \sum_{k=1}^{N_m} M_k R_k t + \frac{X_0 X_\infty e^{k_c t}}{\rho_c [X_\infty - X_0(1 - e^{k_c t})]} \tag{28}$$

There are an infinite number of roots for α_n for corresponding values of n (1 to ∞). The solution will be the sum of all possible solutions, but evaluations of the first 150 roots yielded sufficient convergence and accuracy (Abramowitz and Stegun 1964). The detailed development of the analytical solution (Eqs. 25-28) is illustrated in Supplementary Material (Section B). This is the first use of an analytically derived system of equations to capture both biological and geochemical clogging of piezometers in the field.

5.2 Excess Pore Water Pressure Dissipation Model for Acid Sulfate Soils

The conceptual model developed was presented to represent the different components (biological and chemical clogging) that impact the EPWP trends (Fig. 10). A single vibrating wire piezometer (VWP) was modelled one-dimensionally as a unit cell with radius R, and the radius of the piezometer filter tip was assumed as 20mm based on an array of VWP used in the past by the authors. The relevant field and theoretical model parameter inputs are summarised in Table 3, which are based on the study site at the Shoalhaven floodplain. The field solid-phase bacterial cell density (ρ_c), was calculated using a Helber counting grid and an optical microscope (Novel NMM-820), based on data collected over a year. During laboratory culturing experiments, the initial, maximum cell densities and carrying capacity coefficient were sourced from Indraratna et al. (2020).

The model depicts the exacerbated retardation of EPWP when either individual geochemical or biological clogging only or coupled bio-geochemical clogging was considered. If clogging is ignored, then the EPWP reaches complete dissipation much faster (within 300 days), and the current model then approaches the classical solution of Barron (1948) (Eqs. 19-22). If only geochemical clogging is considered in the model (i.e., ignoring the biological clogging component), retarded dissipation of EPWP was observed, and complete dissipation was observed only after 450 days. When both biological and geochemical clogging was considered in tandem, the greatest extent of retarded pore pressure dissipation was observed, and the EPWP did not completely dissipate even after 700 days. During this time, it was expected that the surrounding porous material of the piezometer filter tip would be clogged extensively, obstructing the groundwater flow paths. On this basis, the extensive porosity reduction due to coupled bio-geochemical clogging could be identified as a significant aspect of PRB longevity.

Figures 11 (a) and (b) show the variation of EPWP with normalised radial distance (r/R_0) for the model at initial (t = 0) and final (t = 800 days) were plotted to examine the

influence of clogging surrounding the piezometer filter tip. Prior to the commencement of clogging (t=0), there was no variation in EPWP between the plots of total clogging and no clogging until r/R_0 = 0.9 (Fig. 11a). This is because the clogging model is time-dependent and initially (t = 0) the EPWP would remain the same for both cases. However, after clogging (t = 800 days), the normalised EPWP reading disparity between the total clogging and without clogging is greatest towards the filter tip and gradually diminishes to zero at the boundary of the unit cell (r/R_0 = 1). This may be because the model assumes the bio-geochemical clogging to be predominant in the proximity of the filter tip ($r/R_0 \rightarrow 0$), and the impact of clogging on the normalised EPWP would be minimal further away from the filter tip ($r/R_0 \rightarrow 1$). Although not within the scope of this paper, the radial variation of EPWP would be more useful when multiple piezometers are used in tandem, where the influence of clogging would impact the measurements of each other.

The time-dependent EPWP is further illustrated in Fig.12 with respect to the normalised radial distance in 3D to represent the complete form of the analytical solution. It demonstrates the general shape (curvature change) of the normalised EPWP in relation to its temporal and spatial distribution (axisymmetric). The analytical solutions (Eqs. 25-28) of the bio-geochemical clogging model incorporating the porosity reduction of the soil/granular annulus surrounding the piezometer represent in a fundamental perspective where clogging leads to malfunctioning piezometers. In practice, this original modelling approach is beneficial to accurately monitor the performance of critical infrastructure as applicable to dams, transportation embankments built on soft soil foundations, and in low-lying reclamation projects in clogging-prone terrains.

5.3 Field Application of the Bio-geochemical Clogging Model

The application of the proposed EPWP dissipation model was demonstrated for a few selected sites at the Ballina bypass along the Pacific Highway (north of Sydney) and the Port of Brisbane. The selected embankments were located in acid sulfate floodplains where piezometer clogging was previously reported (Guy et al. 2006; Indraratna et al. 2018a). The soil properties and parameters for both sites where the EPWP was recorded are provided in Table 4.

5.3.1 Pacific Highway, Ballina Bypass Project, Australia

The Ballina site, located at the Pacific Highway, had a trial embankment constructed over soft to firm estuarine clays (Indraratna et al. 2012). In this site, the soft Holocene clay is about 25 m in thickness, and the soil properties are provided in Table 4. The soft soil foundation was consolidated using conventional fill surcharge, and the EPWP was measured from a vibrating wire piezometer installed at 3.3 m deep at the embankment centreline (Baral et al. 2019).

It is evident that a notable discrepancy in dissipation rate predictions made "with clogging" and "without clogging" exists after approximately 270 days (Fig. 13). This suggests that there is a lag period of about 9 months between installation and evidence of a considerable rate of clogging. When normalised EPWP (u/u_0) had dissipated down to 0.8, there is a discrepancy of 55 days (day 293 – day 348) between the predictions made with and without clogging. This discrepancy continuously increases with time in response to bio-geochemical clogging, which captures the slow dissipation rate. The predicted EPWP curves plotted using the current model show a good agreement with the field data (Fig. 13). The proposed model representing the current bio-geochemical clogging model also provides a significant improvement on the earlier predictions made through more traditional numerical models presented by Yin and Graham (1989) and Indraratna and Redana (2000). The bio-geochemical model closely matches the field observations up until 380 days, where clogging conditions in the field seem to be even worse than the model prediction. In fact, under this extreme condition, the pore pressure

dissipation is insignificant, hence the condition of complete clogging, as observed earlier by Indraratna et al. (2018a).

5.3.2 Port of Brisbane Project, Queensland, Australia

The test embankment at the Port of Brisbane (POB) was raised on upper Holocene soft clay, where the excess pore water pressure (EPWP) was measured at the embankment centreline by a VWP below the groundwater table and normalised in relation to the original static pore pressure. Once again, a notable discrepancy between the predictions made with and without clogging commenced after 230 days (Fig. 14). When u/u_0 had dissipated down to 0.8, there is a discrepancy of 120 days (day 300 – day 420) between the predictions made with and without clogging. The comparison between the prediction models clearly indicates the discrepancy between the predictions made with and without clogging, which increases continuously with time until piezometers are entirely clogged. Although a retarded dissipation rate was observed in field observations, the bio-geochemical clogging model could predict the EPWP with acceptable accuracy for over 2.5 years.

6 Model Limitations

The proposed model is the first use of an analytically derived system of equations to capture both biological and geochemical clogging of piezometers using radial consolidation theory in acidic environments (i.e., low-lying pyritic terrains with iron oxidising bacteria). However, the current mathematical model for radial flow ignores the effects of any vertical or cross flows and assumes that the vibrating wire piezometers Furthermore, the model does not offer a solution for a moving boundary condition (time-dependent) and should be investigated in future research (Feng et al. 2019; Mei et al. 2022).

The model considered the average groundwater chemistry of the selected study site, pH and ion concentrations of the PRB inlet since its construction to assess the overall clogging that

occurs surrounding a piezometer filter tip. While the study was influenced by a specific bacterial strain, namely, *A.Ferrooxidans* as the primary catalyst for bio-geochemical clogging, in reality, other forms of bacterial strains and corresponding changes in bio-geochemical reactivity can lead to deviations from the current mathematical model. Moreover, the reaction rate kinetics used in this model makes a simplification of the mineral precipitation reactions, which are only valid for the selected acidic site in the Shoalhaven floodplain. Rate kinetics is a site-specific parameter determined by the localised groundwater chemistry and other environmental conditions. However, it is assumed that similar site and environmental conditions exist in both selected field applications located along the acidic floodplains of the Eastern coastline of Australia since determining site-specific rate kinetics would be time-consuming for each site. Despite these limitations, the bio-geochemical model provides a significant improvement in the prediction of EPWP dissipation in clogging-prone acidic terrain.

7 Conclusions

This study demonstrated the use of a novel biogeochemical model to predict the retarded dissipation of excess pore water pressure (EPWP) when biological and geochemical clogging occurs in acid sulfate soil. A mathematical model based on radial consolidation was used to define and interpret the extent of clogging surrounding the piezometer tip and to assess its adverse impact on the rate of excess pore pressure dissipation. The following conclusions can be drawn:

1. To capture the impact of clogging, it is vital to incorporate the contributions of the porosity reduction due to the growth of biomass (n_{t_b}) and secondary mineral precipitates (n_{t_c}), and thereby estimate the total porosity reduction (n_t) and assess the associated practical implications. For instance, the model predicted that after about 20

months in an acid sulfate soil, about 65% of the total reduction in porosity of the granular assembly surrounding a piezometer was caused by bacterial (biomass) growth, while the remaining 35% was caused by secondary mineral precipitates. However, in the long-term it is apparent that geochemical clogging may be the predominant clogging mechanism during the decayed bacterial growth phase. The corresponding reductions in hydraulic conductivity due to clogging could be modelled effectively using a normalised Kozeny-Carman equation, through which the hydro-mechanical behaviour of the porous medium could be properly captured.

2. The variation of pH and the levels of contaminant concentrations (mainly Fe and Al) could be considered appropriate indicators to interpret clogging within a pilot-scale PRB located in the Shoalhaven floodplain. For instance, the greatest rise in average piezometric head (i.e. from 0.40 m to 0.85 m) from day 150 to day 790 was observed at the inlet section of PRB, where the smallest average pH (7.1) and the highest dissolved concentrations of Fe (1.53 mg/L) and Al (1.93 mg/L) were measured. These results suggest that the PRB inlet is indeed the most prone to clogging compared to the outlet, as the former is subjected to the most intense geochemical reactivity as the contaminated groundwater enters the PRB. In general, an increasing clogging potential can be corroborated with increased metal concentrations (e.g., Fe and Al) and by a reduced level of the measured pH, while an effective treatment of the contaminated (acidic) groundwater by the PRB's alkaline granular medium represents the opposite behaviour.

3. Considering radial consolidation at a given time, the role of bio-geochemical clogging could be successfully interpreted and quantified by transforming the classical EPWP dissipation curves to capture the individual clogging components (i.e., biological and geochemical parts considered separately or in tandem). The proposed governing

equations (Eqs. 24-28) offer an innovative solution that incorporates the bio-geochemical clogging phenomenon causing retarded EPWP dissipation in the proximity of piezometers, based on field studies such as Ballina Bypass and Port of Brisbane.

4. While the dissipation of EPWP during initial stages corroborates with the classical radial consolidation theory, significantly retarded dissipation was observed after about 260 days for field case studies. This suggests that in such acidic soil conditions, there may be a lag period greater than 9 months between the installation of piezometers and the onset of noticeable rate of clogging by considering the model predictions made in relation to "with clogging" and "without clogging". In a practical perspective, it is imperative to consider well-defined site-specific rate kinetics to improve the accuracy of estimating the time lag period and the corresponding dissipation rate.

Acknowledgements

The authors gratefully acknowledge funding received from the Australian Research Council (ARC) (LP190100439) to support research in this field and the industry partners, Glenys Lugg from Manildra Shoalhaven Starches Pty Ltd and Geoff McIntosh from Douglas Partners. The guidance and support received from Prof Cholachat Rujikiatkamjorn and Dr Ana Heitor throughout the research is greatly appreciated. The authors would like to appreciate the support and assistance provided by the technical staff at UOW during fieldwork. The authors would also like to acknowledge the efforts of UTS technical staff.

Notation

The following symbols are used in this paper:

u	excess pore water pressure (EPWP)
u_0	initial excess pore water pressure
r	radial distance
R_0	radius of the axisymmetric unit cell
t	time
z	depth
c_v	coefficient of vertical consolidation
c_h	coefficient of horizontal consolidation
k	hydraulic conductivity
K_0	initial hydraulic conductivity
k_h	horizontal coefficient of permeability
m_v	coefficient of volume compressibility
γ_w	unit weight of water
e_0	initial void ratio
C_c	compression index
n_t	porosity at time t
n_0	initial porosity
n_{t_b}	reduction in porosity due to the growth of biomass
n_{t_c}	reduction in porosity due to secondary mineral precipitates
N_m	number of minerals
R_k	overall reaction rate for the mineral
M_k	mineral molar volume
Xs	solid phase concentration of bacterial cells (based on Monod's kinetics)
ρ_c	solid phase biomass density
X_0	initial concentration of bacterial cells
X_∞	maximum concentration of bacterial cells
k_c	carrying capacity coefficient
k_r	kinetic rate coefficient
r_k	reaction rate of each component
K_{eq}	solubility constant for each reaction
$\emptyset_m$	volume fraction of mineral

Competing Interests

The authors declare there are no competing interests.

Data Availability Statement

All data used in the study are available from the corresponding author by request.

Field methodology, analytical framework used in the study are described in the paper.

References

Abramowitz, M and Stegun, IA 1964, *Handbook of Mathematical Functions with Formulas, Graphs, and Mathematical Tables*, U.S. Government Printing Office.

ANZECC 2000, 'Australian and New Zealand guidelines for fresh and marine water quality', *Australian and New Zealand Environment and Conservation Council and Agriculture and Resource Management Council of Australia and New Zealand, Canberra*, pp. 1-103.

Arulrajah, A, Bo, M, Leong, M and Disfani, M 2013, 'Piezometer measurements of prefabricated vertical drain improvement of soft soils under land reclamation fill', *Engineering Geology*, vol. 162, pp. 33-42.

Arulrajah, A, Nikraz, H and Bo, M 2004, 'Factors affecting field instrumentation assessment of marine clay treated with prefabricated vertical drains', *Geotextiles and Geomembranes*, vol. 22, no. 5, pp. 415-37.

ASTM 2020, *Standard Practice for Pre-Installation Acceptance Testing of Vibrating Wire Piezometers, ASTM D7764-20*, American Society for Testing and Materials (ASTM) International, West Conshohocken, PA.

Athuraliya, S 2017, 'Investigation of Bio-Geochemical Clogging In Low-Lying Permeable Reactive Barriers', Honours thesis, University of Wollongong, Wollongong.

Baker, BJ and Banfield, JF 2003, 'Microbial communities in acid mine drainage', *FEMS Microbiology Ecology*, vol. 44, no. 2, pp. 139-52.

Baral, P, Indraratna, B, Rujikiatkamjorn, C, Kelly, R and Vincent, P 2021, 'Consolidation by Vertical Drains beneath a Circular Embankment under Surcharge and Vacuum Preloading', *Journal of Geotechnical and Geoenvironmental Engineering*, vol. 147, no. 8, p. 05021004.

Baral, P, Rujikiatkamjorn, C, Indraratna, B, Leroueil, S and Yin, JH 2019, 'Radial Consolidation Analysis Using Delayed Consolidation Approach', *Journal of Geotechnical and Geoenvironmental Engineering*, vol. 145, no. 10, p. 04019063.

Barron, RA 1948, 'Consolidation of fine-grained soils by drain wells', *Transactions of the American Society of Civil Engineers (ASCE)*, vol. 113, no. 1, pp. 718-54.

Beaven, RP, Cox, SE and Powrie, W 2007, 'Operation and Performance of Horizontal Wells for Leachate Control in a Waste Landfill', *Journal of Geotechnical and Geoenvironmental Engineering*, vol. 133, no. 8, pp. 1040-7.

Bergado, D, Manivannan, R and Balasubramaniam, A 1996, 'Filtration criteria for prefabricated vertical drain geotextile filter jackets in soft Bangkok clay', *Geosynthetics International*, vol. 3, no. 1, pp. 63-83.

Bigham, JM and Nordstrom, DK 2000, 'Iron and Aluminum Hydroxysulfates from Acid Sulfate Waters', *Reviews in Mineralogy and Geochemistry*, vol. 40, no. 1, pp. 351-403.
Bo, MW and Choa, V 2004, *Reclamation and ground improvement*, Thomson Learning Asia.
Bustos Medina, DA, Van Den Berg, GA, Van Breukelen, BM, Juhasz-Holterman, M and Stuyfzand, PJ 2013, 'Iron-hydroxide clogging of public supply wells receiving artificial recharge: near-well and in-well hydrological and hydrochemical observations', *Hydrogeology Journal*, vol. 21, no. 7, pp. 1393-412.
Chen-Charpentier, B 1999, 'Numerical simulation of biofilm growth in porous media', *Journal of computational and applied mathematics*, vol. 103, no. 1, pp. 55-66.
Chu, J, Bo, MW and Choa, V 2004, 'Practical considerations for using vertical drains in soil improvement projects', *Geotextiles and Geomembranes*, vol. 22, no. 1, pp. 101-17.
Cooke, AJ and Rowe, RK 2008, 'Modelling landfill leachate-induced clogging of field-scale test cells (mesocosms)', *Canadian Geotechnical Journal*, vol. 45, no. 11, pp. 1497-513.
Deed, MER and Preene, M 2015, 'Managing the clogging of groundwater wells', in *Geotechnical Engineering for Infrastructure and Development*, pp. 2787-92.
Dent, DL and Pons, LJ 1995, 'A world perspective on acid sulphate soils', *Geoderma*, vol. 67, no. 3, pp. 263-76.
Dibiagio, E 1977, 'Field Instrumentation - A Geotechnical Tool', *Norwegian Geotechnical Institute Publication*, no. 115, pp. 29-40.
Dunnicliff, J 1993, *Geotechnical Instrumentation for Monitoring Field Performance*, John Wiley & Sons, New York.
Dunnicliff, J 2008, 'Geotechnical Instrumentation News', *Geotechnical News*, vol. 26, no. 1, pp. 31-2.
Easton, C and Springer, R 2016, 'What's in Your Piezometer? Evaluating and Maintaining Piezometers, Relief Wells, and Drains', *In Proceedings of Association of State Dam Safety Officials National Conference, Dam Safety 2016*, Philadelphia.
Feng, J, Ni, P and Mei, G 2019, 'One-dimensional self-weight consolidation with continuous drainage boundary conditions: Solution and application to clay-drain reclamation', *International Journal for Numerical and Analytical Methods in Geomechanics*, vol. 43, no. 8, pp. 1634-52.
Fleming, I, Rowe, R and Cullimore, DR 1999, 'Field observations of clogging in a landfill leachate collection system', *Canadian Geotechnical Journal*, vol. 36, no. 4, pp. 685-707.
Fleming, IR and Rowe, RK 2004, 'Laboratory studies of clogging of landfill leachate collection and drainage systems', *Canadian Geotechnical Journal*, vol. 41, no. 1, pp. 134-53.
Gibert, O, Assal, A, Devlin, H, Elliot, T and Kalin, RM 2019, 'Performance of a field-scale biological permeable reactive barrier for in-situ remediation of nitrate-contaminated groundwater', *Science of The Total Environment*, vol. 659, pp. 211-20.
Guy, E, Calhoun, T, Alford, G, Barry, C and Rogers, A 2006, 'Relief wells rehabilitation at Alum Creek and Dillon dams', *In Proceedings of Annual Conference Proceedings, Association of State Dam Safety Officials*, pp. 1-21.
Hanna, TH 1985, 'Field instrumentation in geotechnical engineering'.
Houben, GJ 2003, 'Iron oxide incrustations in wells. Part 1: genesis, mineralogy and geochemistry', *Applied Geochemistry*, vol. 18, no. 6, pp. 927-39.
Hvorslev, M 1951, *Time lag and soil permeability in ground-water observations*, Bulletin No. 36, Waterways Experiment Station, Corps of Engineers, US Army, Vicksburg, Mississippi.
Indraratna, B, Balasubramaniam, AS and Balachandran, S 1992, 'Performance of Test Embankment Constructed to Failure on Soft Marine Clay', *Journal of geotechnical engineering*, vol. 118, no. 1, pp. 12-33.
Indraratna, B, Baral, P, Ameratunga, J and Kendaragama, B 2017, 'Potential Biological and Chemical Clogging of Piezometer Filters in Acid Sulphate Soil', *Australian Geomechanics Journal*, vol. 52, no. 2, pp. 79-85.
Indraratna, B, Baral, P, Ameratunga, J, Kendaragama, B and Athuraliya, S 2018a, 'Potential Biological and Geochemical Clogging of Vibrating Wire Piezometers in Low-lying Acid Sulphate Soil', *In Proceedings of Australian National Committee on Large Dams (ANCOLD) Conference*, Melbourne, Victoria, October, 2018, vol. Paper ID: 6 (5B;).

Indraratna, B, Baral, P, Rujikiatkamjorn, C and Perera, D 2018b, 'Class A and C predictions for Ballina trial embankment with vertical drains using standard test data from industry and large diameter test specimens', *Computers and Geotechnics*, vol. 93, pp. 232-46.

Indraratna, B, Medawela, S, Rowe, RK, Thamwattana, N and Heitor, A 2020, 'Biogeochemical Clogging of Permeable Reactive Barriers in Acid-Sulfate Soil Floodplain', *Journal of Geotechnical and Geoenvironmental Engineering*, vol. 146, no. 5, p. 04020015.

Indraratna, B, Pathirage, PU, Rowe, RK and Banasiak, L 2014, 'Coupled hydro-geochemical modelling of a permeable reactive barrier for treating acidic groundwater', *Computers and Geotechnics*, vol. 55, pp. 429-39.

Indraratna, B and Redana, IW 2000, 'Numerical modeling of vertical drains with smear and well resistance installed in soft clay', *Canadian Geotechnical Journal*, vol. 37, no. 1, pp. 132-45.

Indraratna, B, Rujikiatkamjorn, C, Kelly, R and Buys, H 2012, 'Soft soil foundation improved by vacuum and surcharge loading', *Proceedings of the Institution of Civil Engineers-Ground Improvement*, vol. 165, no. 2, pp. 87-96.

Karimian, N, Johnston, SG and Burton, ED 2018, 'Iron and sulfur cycling in acid sulfate soil wetlands under dynamic redox conditions: A review', *Chemosphere*, vol. 197, pp. 803-16.

Kelly, R, Sloan, S, Pineda, J, Kouretzis, G and Huang, J 2018, 'Outcomes of the Newcastle symposium for the prediction of embankment behaviour on soft soil', *Computers and Geotechnics*, vol. 93, pp. 9-41.

Li, L, Benson, CH and Lawson, EM 2006, 'Modeling porosity reductions caused by mineral fouling in continuous-wall permeable reactive barriers', *Journal of contaminant hydrology*, vol. 83, no. 1, pp. 89-121.

Little, A and Vail, A 1960, 'Some developments in the measurement of pore pressure', *In Proceedings of Proceedings, Conference on Pore Pressure and Suction in Soils*, Butterworth, London, pp. 75-80.

Liu, GB, Ng, CW and Wang, ZW 2005, 'Observed Performance of a Deep Multistrutted Excavation in Shanghai Soft Clays', *Journal of Geotechnical and Geoenvironmental Engineering*, vol. 131, no. 8, pp. 1004-13.

Liu, HL, Ng, CWW and Fei, K 2007, 'Performance of a Geogrid-Reinforced and Pile-Supported Highway Embankment over Soft Clay: Case Study', *Journal of Geotechnical and Geoenvironmental Engineering*, vol. 133, no. 12, pp. 1483-93.

Macdonald, DG and Clark, RH 1970, 'The oxidation of aqueous ferrous sulphate by thiobacillus ferrooxidans', *The Canadian Journal of Chemical Engineering*, vol. 48, no. 6, pp. 669-76.

Marsland, A 1973, 'Instrumentation of flood defense banks along the river Thames', *In Proceedings of Proceeding of the British Geotechnical Society Symposium on Field Instrumentation in Geotechnical Engineering*, London, pp. 297-303.

Mclaughlan, RG, Knight, MJ and Stuetz, RM 1993, *Fouling and Corrosion of Groundwater Wells—A Research Study*, Research publication (University of Technology, Sydney. National Centre for Groundwater Management), Sydney : National Centre for Groundwater Management, University of Technology, 1993, Sydney.

Medawela, S and Indraratna, B 2020, 'Computational modelling to predict the longevity of a permeable reactive barrier in an acidic floodplain', *Computers and Geotechnics*, vol. 124.

Medawela, S, Indraratna, B, Athuraliya, S, Lugg, G and Nghiem, LD 2022, 'Monitoring the performance of permeable reactive barriers constructed in acid sulfate soils', *Engineering Geology*, vol. 296.

Medawela, S, Indraratna, B and Rowe, RK 2023, 'The reduction in porosity of permeable reactive barriers due to bio-geochemical clogging caused by acidic groundwater flow', *Canadian Geotechnical Journal*, vol. 60, no. 2, pp. 151-65.

Mehdizadeh, A and Fakharian, K 2015, 'Field instrumentation of a preloading project with prefabricated vertical drains', paper presented to FMGM 2015: Proceedings of the 9th Symposium on Field Measurements in Geomechanics, Sydney, 9-11 September.

Mei, G, Feng, J, Xu, M and Ni, P 2022, 'Estimation of Interface Parameter for One-Dimensional Consolidation with Continuous Drainage Boundary Conditions', *International Journal of Geomechanics*, vol. 22, no. 3.

Monod, J 1949, 'The growth of bacterial cultures', *Annual Reviews in Microbiology*, vol. 3, no. 1, pp. 371-94.
Nguyen, T, Indraratna, B, Rujikiatkamjorn, C and Xu, B 2022, 'Evaluation on the performance of field embankment testing biodegradable drains based on spectral method analysis', *In Proceedings of 20th International Conference of Soil Mechanics and Geotechnical Engineering (ICSMGE)*.
Nordstrom, DK 1982, *Aqueous pyrite oxidation and the consequent formation of secondary iron minerals*, Soil Science Society of America, Madison, WI.
Puls, RW, Blowes, DW and Gillham, RW 1999, 'Long-term performance monitoring for a permeable reactive barrier at the U.S. Coast Guard Support Center, Elizabeth City, North Carolina', *J. Hazard. Mater.*, vol. 68, p. 109.
Ralph, DE and Stevenson, JM 1995, 'The role of bacteria in well clogging', *Water Research*, vol. 29, no. 1, pp. 365-9.
Reddi, LN, Ming, X, Hajra, MG and Lee, IM 2000, 'Permeability Reduction of Soil Filters due to Physical Clogging', *Journal of Geotechnical and Geoenvironmental Engineering*, vol. 126, no. 3, pp. 236-46.
Regmi, G, Indraratna, B and Nghiem, L 2009, 'Long-term Performance of a Permeable Reactive Barrier in Acid Sulphate Soil Terrain', *Water, Air & Soil Pollution: Focus*, vol. 9, no. 5/6, pp. 409-19.
Regmi, G, Indraratna, B, Nghiem, LD, Golab, AN and Guru Prasad, B 2011, 'Treatment of Acidic Groundwater in Acid Sulfate Soil Terrain Using Recycled Concrete: Column Experiments', *Journal of Environmental Engineering*, vol. 137, no. 6, pp. 433-43.
Ren, Z, Lu, Q, Liu, K, Ni, P and Mei, G 2022, 'Model-scale tests to examine water pressures acting on potentially buoyant underground structures in clay strata', *Journal of Rock Mechanics and Geotechnical Engineering*, vol. 14, no. 3, pp. 861-72.
Ren, Z, Ni, P and Mei, G 2020, 'Time Effect of Buoyant Force Reduction for Underground Structures in Clays: Model Test and Case Study', *International Journal of Geomechanics*, vol. 20, no. 10.
Rowe, R and Fleming, I 1998, 'Estimating the time for clogging of leachate collection systems', *In Proceedings of 3rd International Congress on Environmental Geotechnics*, Lisbon, vol. 1, pp. 23 – 8.
Rowe, RK, Armstrong, MD and Cullimore, DR 2000, 'Mass loading and the rate of clogging due to municipal solid waste leachate', *Canadian Geotechnical Journal*, vol. 37, no. 2, pp. 355-70.
Shuler, ML and Kargi, F 2002, *Bioprocess Engineering: Basic Concepts*, Second edn, Prentice Hall PTR, Upper Saddle River, New Jersey.
Singer, PC and Stumm, W 1970, 'Acidic mine drainage: The rate-determining step', *Science*, vol. 167, p. 1121.
Smith, J and Melville, MD 2004, 'Iron monosulfide formation and oxidation in drain-bottom sediments of an acid sulfate soil environment', *Applied Geochemistry*, vol. 19, no. 11, pp. 1837-53.
Steefel, CI and Lasaga, AC 1994, 'A coupled model for transport of multiple chemical species and kinetic precipitation/dissolution reactions with application to reactive flow in single phase hydrothermal systems', *American Journal of science*, vol. 294, no. 5, pp. 529-92.
Sterpejkowicz-Wersocki, W 2014, 'Problem of Clogging in Drainage Systems in the Examples of the Żur and Podgaje Dams', *Archives of Hydro-Engineering and Environmental Mechanics*, vol. 61, no. 3-4, pp. 183-92.
Take, W and Bolton, M 2003, 'Tensiometer saturation and the reliable measurement of soil suction', *Geotechnique*, vol. 53, no. 2, pp. 159-72.
Vangulck, JF and Rowe, RK 2008, 'Parameter estimation for modelling clogging of granular medium permeated with leachate', *Canadian Geotechnical Journal*, vol. 45, no. 6, pp. 812-23.
Wang, M and Zhou, L 2012, 'Simultaneous oxidation and precipitation of iron using jarosite immobilized Acidithiobacillus ferrooxidans and its relevance to acid mine drainage', *Hydrometallurgy*, vol. 125-126, pp. 152-6.
Yangiev, A, Omarova, G, Yunusova, F, Adjimuratov, D and Risalieva, A 2021, 'The study results of the filtration process in the ground dams body and its chemical effect on piezometers', *In Proceedings of E3S Web of Conferences*, vol. 264, p. 03014.
Yin, J-H and Graham, J 1989, 'Viscous–elastic–plastic modelling of one-dimensional time-dependent behaviour of clays', *Canadian Geotechnical Journal*, vol. 26, no. 2, pp. 199-209.

Yu, Y and Rowe, RK 2012, 'Modelling leachate-induced clogging of porous media', *Canadian Geotechnical Journal*, vol. 49, no. 8, pp. 877-90.

List of Tables

Table 1: Average groundwater chemistry recorded from study site (Indraratna et al. 2020)

Groundwater Parameter	Average Value
pH	3.7
ORP	530 mV
Na^+	467 mg/L
K^+	48 mg/L
Ca^{2+}	142 mg/L
Mg^{2+}	147 mg/L
Al^{3+}	54 mg/L
Fe^{3+}	49 mg/L
Fe^{2+}	91 mg/L
Cl^-	815 mg/L
SO_4^{2-}	1313 mg/L

Table 2: Kinetic rate coefficients (k_r) from previous literature (Medawela and Indraratna 2020)

Mineral Type	**Kinetic rate coefficients (k_r) of mineral**	**Kinetic rate coefficients (k_r) mol.L^{-1}s^{-1}**	
		Laboratory	Field
Fe^{3+} bearing	$Fe(OH)_3$	8.98E-08	2.81E-08
Fe^{3+} bearing	$FeO(OH)$	8.49E-08	2.56E-08
Fe^{3+} bearing	Fe_2O_3	7.81E-08	2.62E-08
Al^{3+} bearing	$Al(OH)_3$	3.03E-07	8.98E-08
Chemical/ abiotic ferrous oxidation	$Fe^{2+}_{(aq)}$ abiotic	5.62E-08	1.97E-08
Biotic ferrous oxidation	$Fe^{2+}_{(aq)}$ biotic	3.09E-07	9.82E-08

Table 3: Field and Model Parameters

ρ_c	X_0	X_∞	k_c	n_0	m_v	K_0	γ_w
cells/cm^3	cells/cm^3	cells/cm^3	d^{-1}	-	m^2/N	m/d	N/m^3
1.0×10^9	7.0×10^7	2.95×10^8	0.009	0.69	0.002399	0.9565	9810

(Source: Data from Indraratna et al. 2020)

Table 4: Soil properties for Ballina Bypass and Port of Brisbane (POB)

Site	e_0	$Cc/(1+e_0)$	m_v (m^2/kN)	k (m/s)
Ballina	2.9	0.36	0.00212	1.0×10^{-9}
Port of Brisbane	2.6	0.18	0.00161	3.3×10^{-10}

(Source: Data from Baral et al. 2019 and Indraratna et al. 2018b)

List of Figures

Figure 12: Conceptual 3D Plot variation of the Bio-geochemical Model

Figure 13: Comparison of excess pore water pressure dissipation recorded by piezometer (P1) on Ballina Bypass project with the current and existing models (Source: Field data from Indraratna et al. 2018b)

Figure 14: Comparison of excess pore water pressure dissipation recorded by a vibrating wire piezometer at Port of Brisbane (POB) with the current model (Source: Field data from Indraratna et al. 2018b)

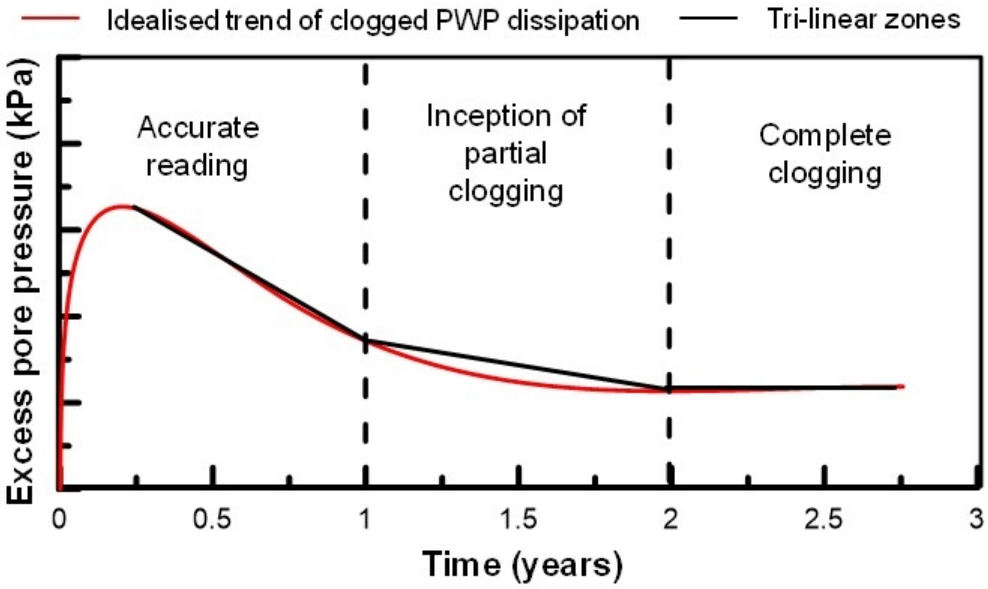

Figure 1: Trilinear trend for excess pore water pressure (EPWP) dissipation (after Indraratna et al. 2017)

112x69mm (150 x 150 DPI)

Figure 2: Malfunctioned instrumentation extracted from field sites located in acid sulfate soils: (a) Multi-parameter sensor from Shoalhaven floodplain; (b) Standpipe filter tip from Shoalhaven floodplain; (c) Vibrating wire piezometer from Ballina, NSW and its (d) mineral precipitation on sensor surface and (d) filter tip

231x93mm (150 x 150 DPI)

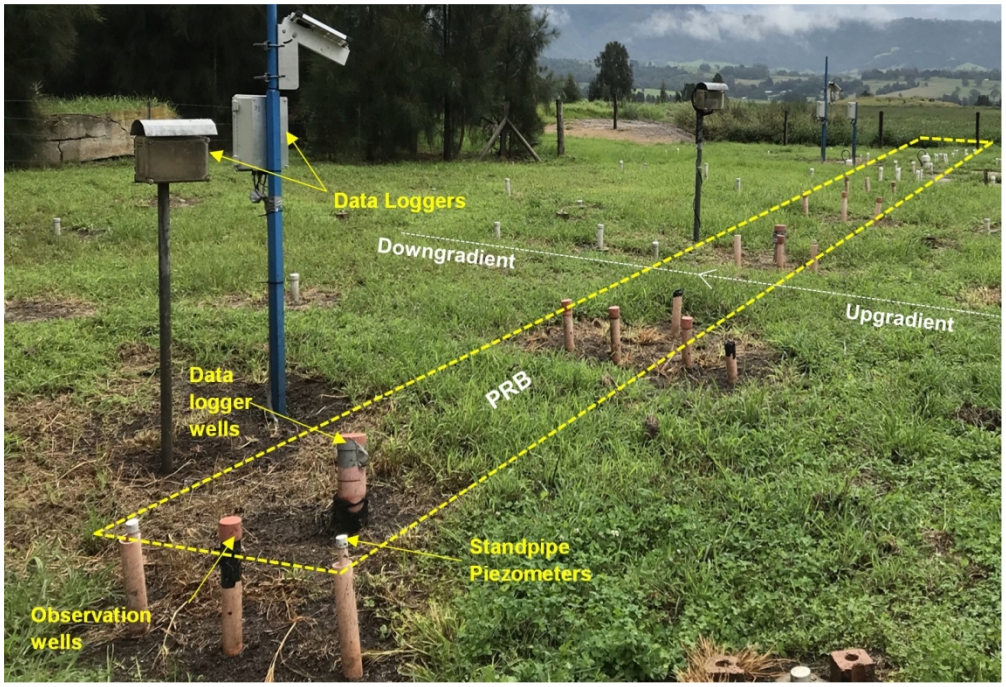

Figure 3: Study site (Permeable reactive barrier-PRB) located in acid sulfate terrain, Shoalhaven floodplain, NSW

270x183mm (150 x 150 DPI)

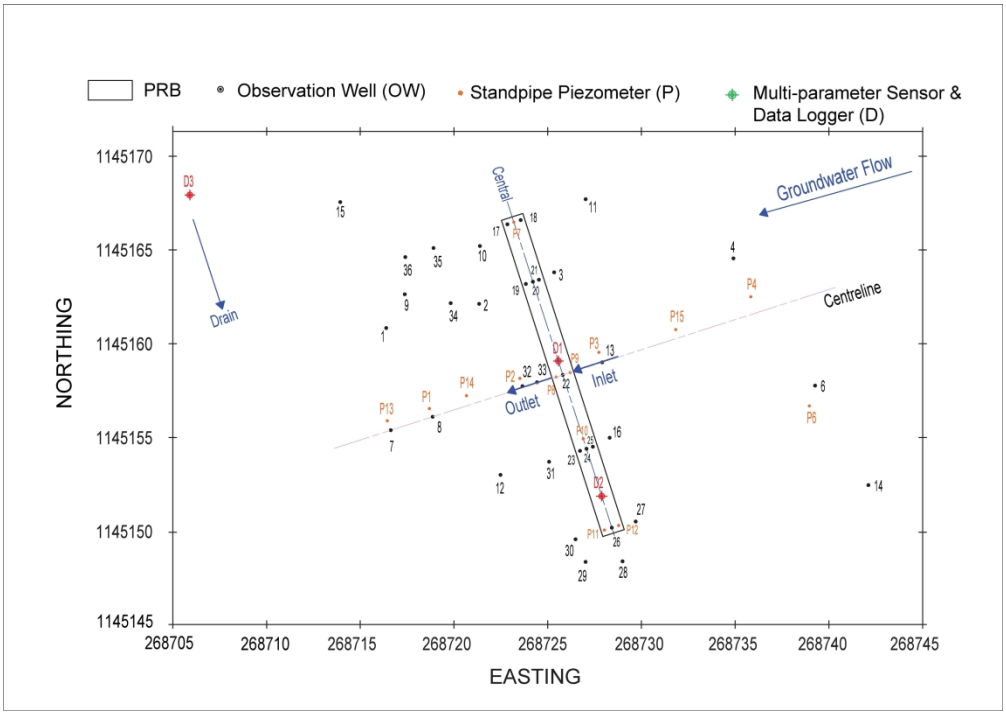

Figure 4: Layout of the monitoring instruments installed at the PRB site in the Shoalhaven floodplain, NSW

297x209mm (300 x 300 DPI)

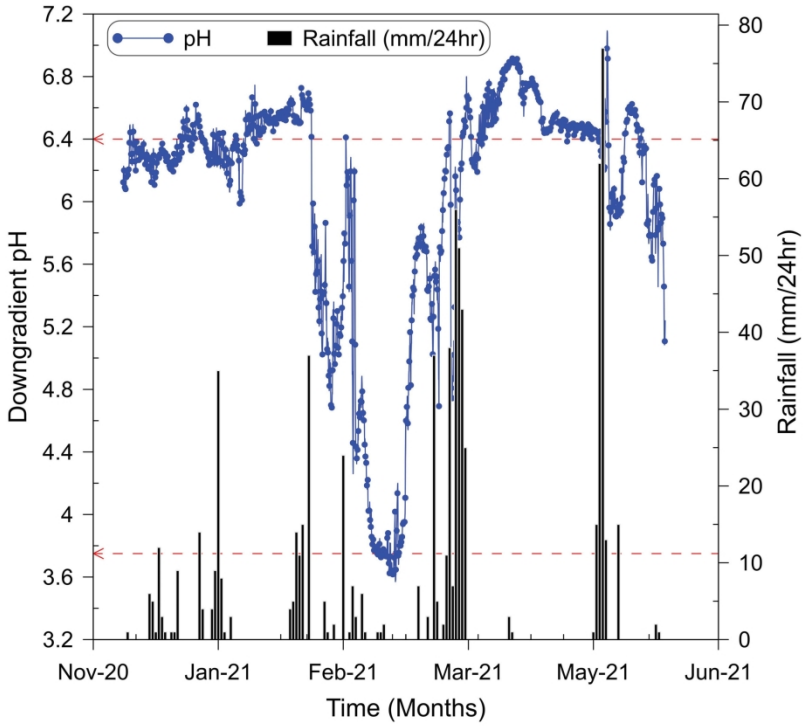

Figure 5: Rainfall and pH variation measured at the study site (pH measured by multi-parameter sensor located at in the downgradient near the creek)

209x297mm (300 x 300 DPI)

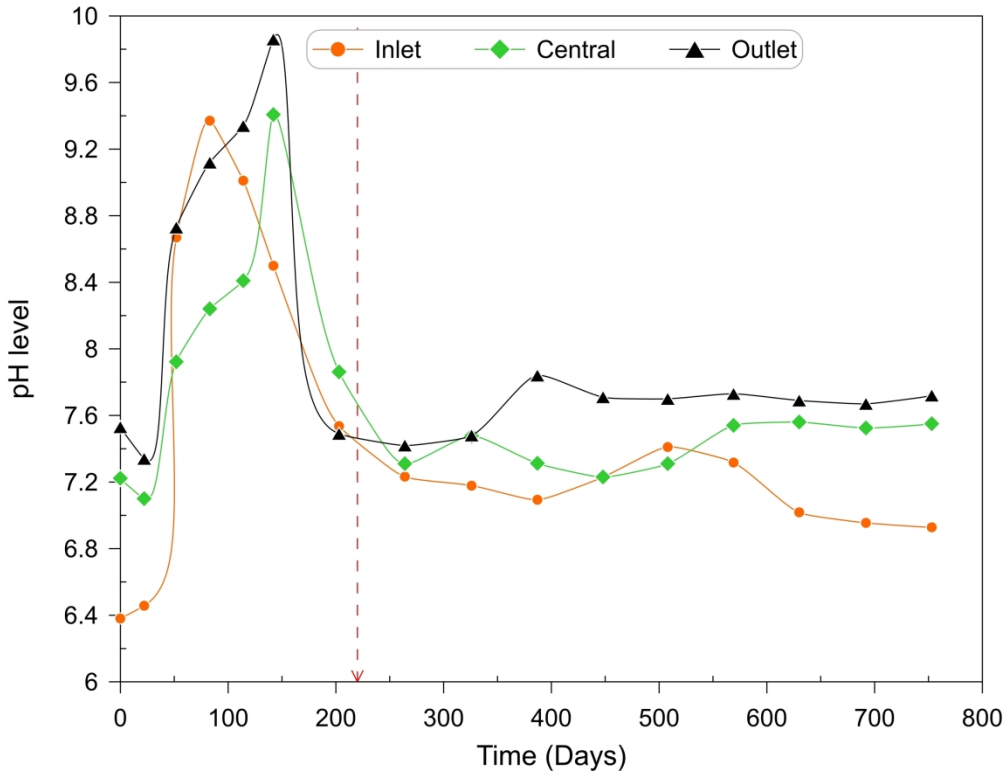

Figure 6: Variations of pH at different sections [Inlet (0 m – 0.4 m), central (0.4 m – 0.8 m) and outlet (0.8 – 1.2 m) sections] along the flow path through the PRB (Source: Field data from Medawela et al. 2022)

229x176mm (300 x 300 DPI)

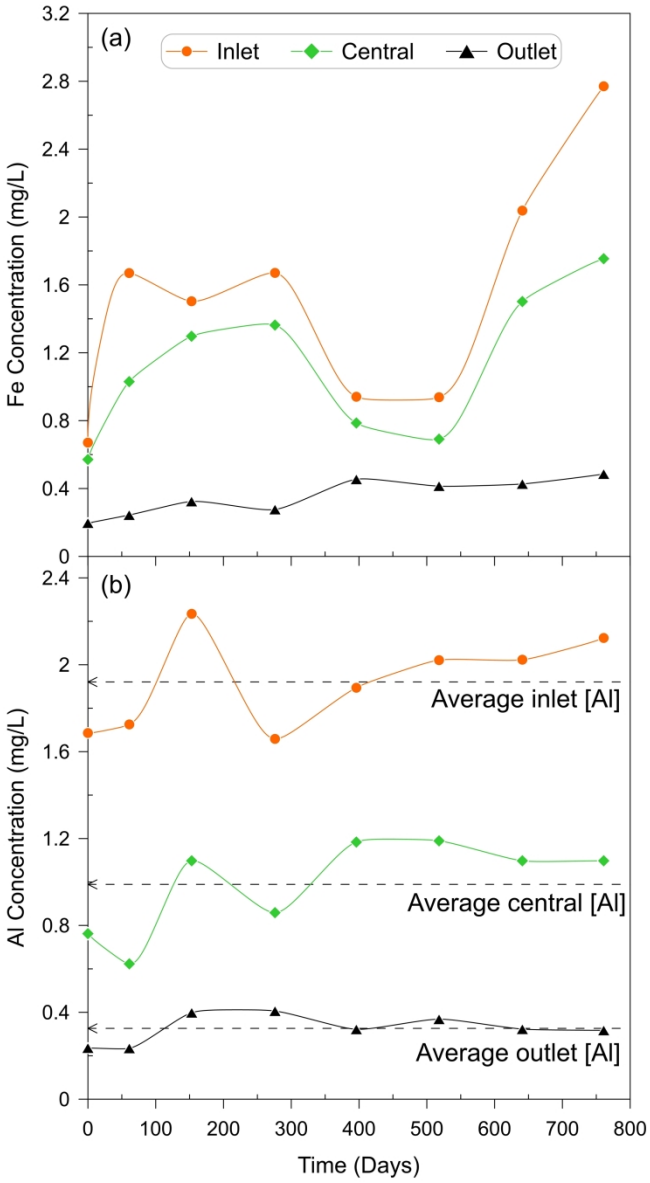

Figure 7: Variations in concentrations of Fe and Al (mg/L) at different sections along the flow path within the PRB (a) Fe and (b) Al (Source: Field data from Medawela et al. 2022)

181x337mm (300 x 300 DPI)

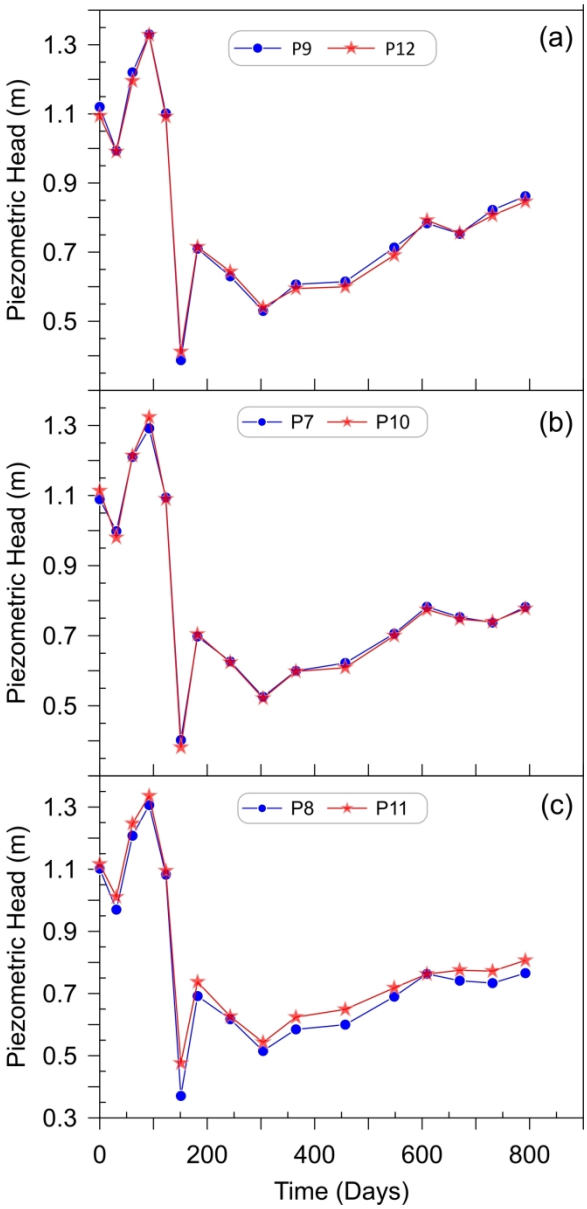

Figure 8: Piezometric head within the PRB at: (a) inlet (0 m – 0.4 m); (b) central (0.4 m – 0.8 m); (c) outlet (0.8 – 1.2 m) (Source: Field data from Medawela et al. 2022)

131x270mm (300 x 300 DPI)

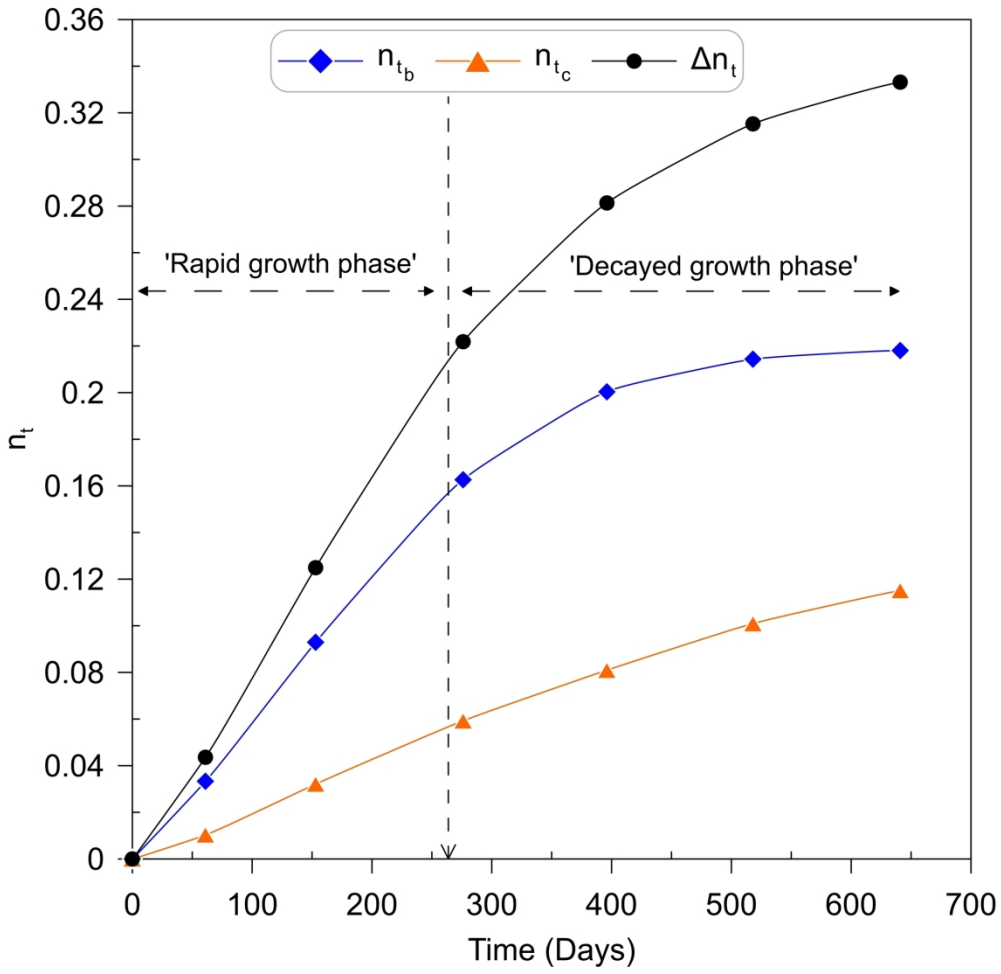

Figure 9: Model predictions on the effect of biological and geochemical clogging in reducing the total porosity for the PRB inlet

181x175mm (300 x 300 DPI)

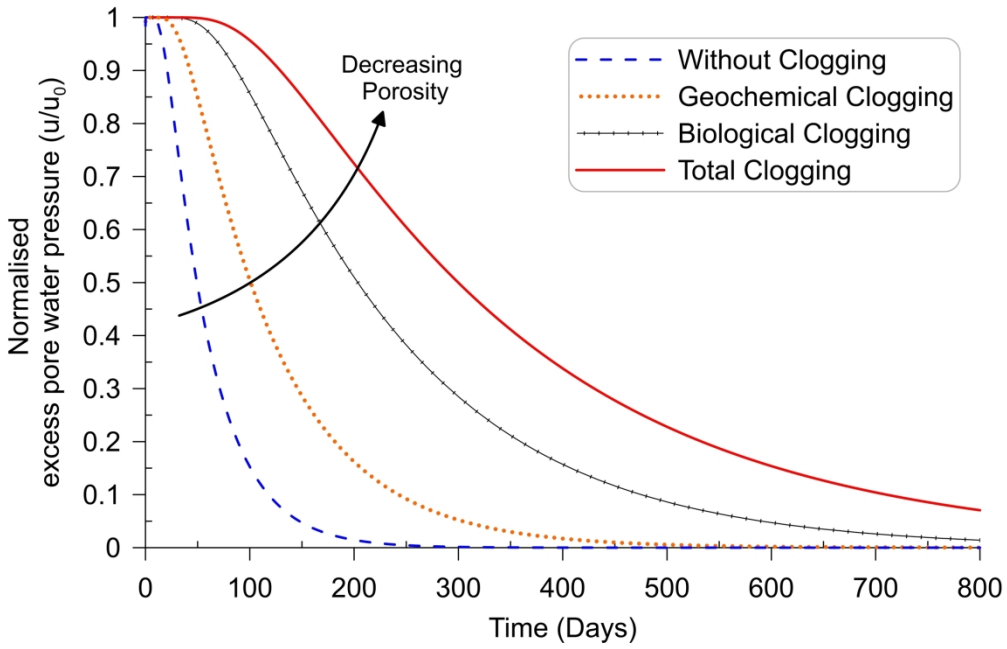

Figure 10: Theoretical representation of model Excess PWP dissipation (At r= 0.02 m) when implications of biological and geochemical clogging are considered

205x132mm (300 x 300 DPI)

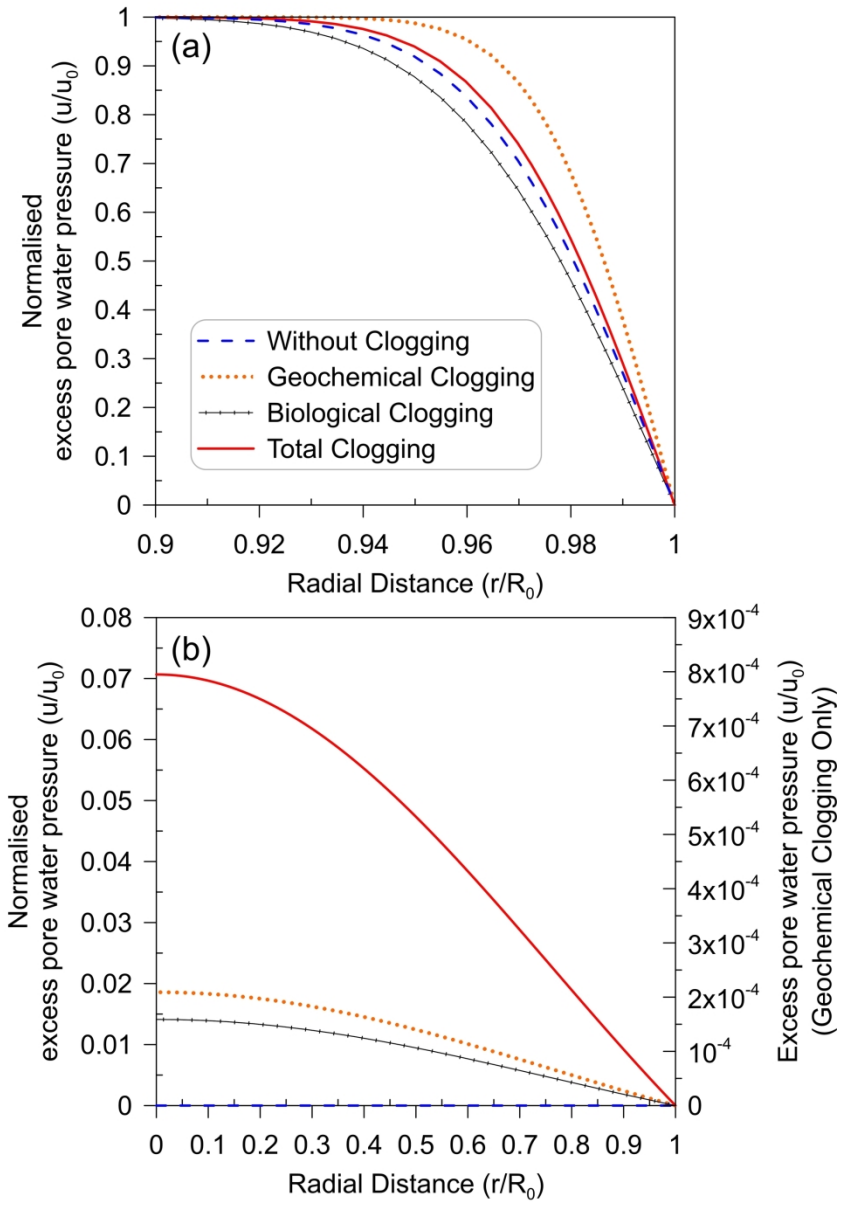

Figure 11: EPWP vs. Radial distance (r/R_0) variation at: (a) t = 0 days; (b) t = 800 days. (Model domain: 0<r≤1)

176x253mm (300 x 300 DPI)

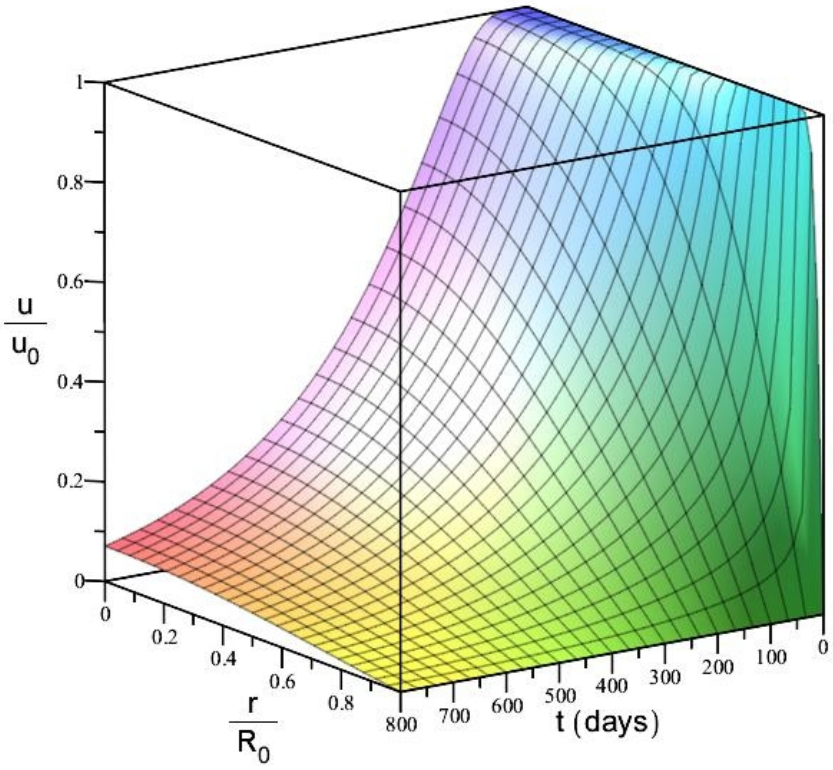

Figure 12: Conceptual 3D Plot variation of the Bio-geochemical Model

246x246mm (72 x 72 DPI)

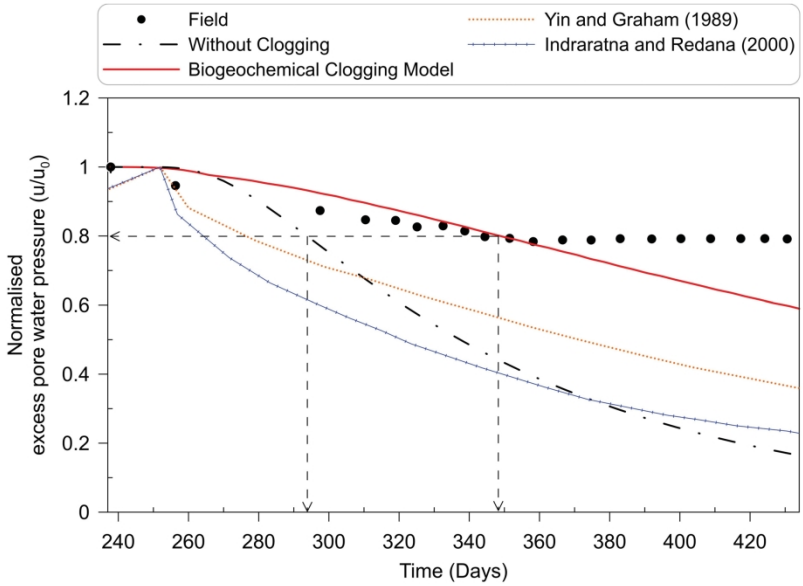

Figure 13: Comparison of excess pore water pressure dissipation recorded by piezometer (P1) on Ballina Bypass project with the current and existing models (Source: Field data from Indraratna et al. 2018b)

209x297mm (300 x 300 DPI)

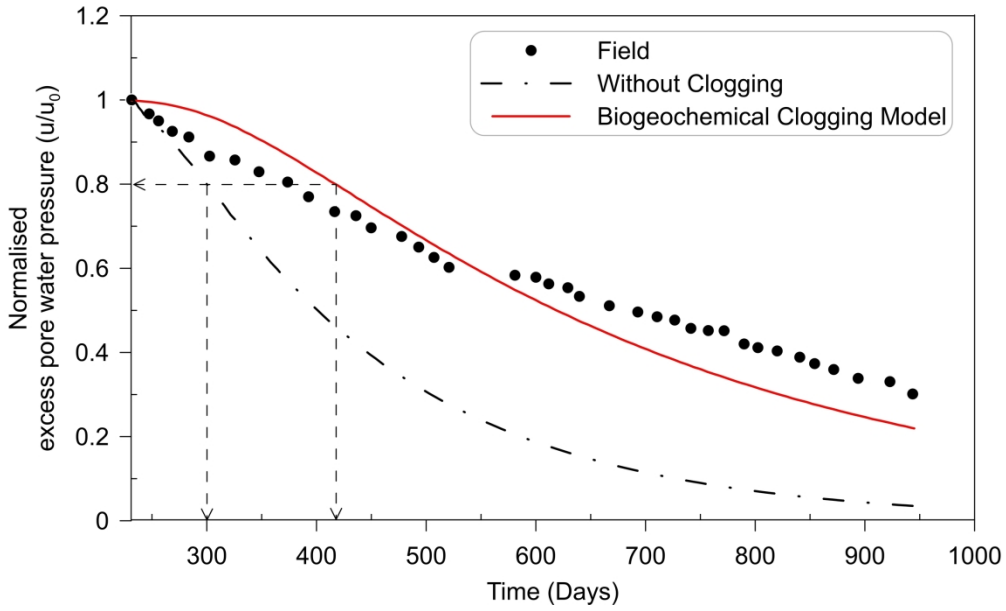

Figure 14: Comparison of excess pore water pressure dissipation recorded by a vibrating wire piezometer at Port of Brisbane (POB) with the current model (Source: Field data from Indraratna et al. 2018b)

230x139mm (300 x 300 DPI)